Strengthening of steel I-Section girder web with depth discontinuity against localized buckling

Amin H. Almasri
Jordan University of Science and Technology, Jordan
ahalmasri@just.edu.jo, https://orcid.org/0000-0002-5425-7704

Mohammad Nadeem Akhtar
Fahad Bin Sultan University, Tabuk, Saudi Arabia
nakhtar@fbsu.edu.sa, https://orcid.org/0000-0002-7806-1896

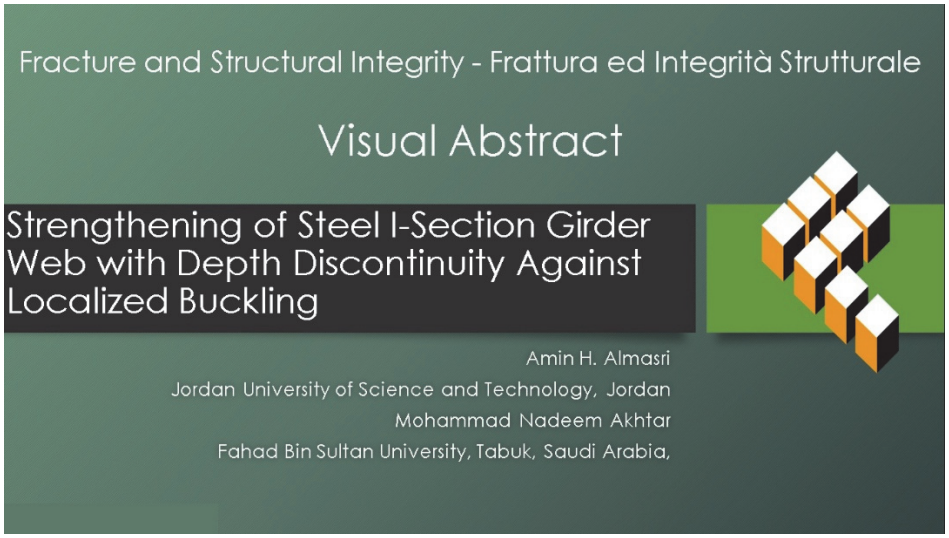

Citation: Almasri, A. H., Akhtar, M. N., Strengthening of steel I-Section girder web with depth discontinuity against localized buckling, Fracture and Structural Integrity, 74 (2025) 342-357.

Received: 15.06.2025
Accepted: 06.09.2025
Published: 11.09.2025
Issue: 10.2025

KEYWORDS. Steel, Web buckling, Stepped girders, Finite element method.

INTRODUCTION

Steel I-section girders and beams are widely used in the construction industry due to their high strength-to-weight ratio, durability, and ease of fabrication. However, these structural members are susceptible to phenomena such as web buckling, which can significantly reduce their load-carrying capacity and compromise the overall structural integrity. Web buckling occurs when the web of a steel I-section girder or beam experiences compressive stresses that exceed its critical buckling stress. It can be attributed to several factors, including:

1. Eccentricity of Load: When the load is applied to the girder with an eccentricity, additional stresses are added to it due to this eccentricity, causing it to reach the buckling capacity faster.

2. Shear Lag: Shear lag is a phenomenon where the stress distribution in the web is not uniform due to the non-uniform distribution of shear forces, leading to localized stress concentrations, such as those around bolt holes. It can add complexity to the stress state of the web and, therefore, could lower the buckling capacity of the web.

3. Web Thickness: Slender webs, characterized by a large height-to-thickness ratio, are more susceptible to buckling due to their lower flexural stiffness.

4. Web Openings: The presence of web openings, such as access holes or cutouts, can significantly reduce the web's effective area and stiffness, making it more prone to buckling.

Steel web buckling of I-section beams and girders is a critical failure mode that must be thoroughly understood for the safe and efficient design. The behavior of steel web elements under various loading conditions and material properties has been extensively studied. There are different types of web buckling, like shear buckling, lateral buckling along the whole length of the girder, and local web compression buckling. They are illustrated in Fig. 1. Several techniques can be employed to prevent or control web buckling in steel plate girders, such as using web stiffeners (vertical or longitudinal) or increasing the thickness of the web. Such techniques increase the web flexural stiffness and resistance to buckling. Steel I-girders often can be loaded beyond the web buckling load predicted by the classical plate buckling theory. It is because the web plate is framed by flanges and transverse stiffeners, allowing stress redistribution.

(a) (b) (c)

Figure 1: Different types of steel I-section beam web buckling, (a) shear buckling, (b) web lateral buckling along the whole span, and (c) local web buckling.

Steel beams with varying section depths have become more common in recent years. They are used to reduce material, reduce self-weight, provide room access for utility services, or for aesthetic reasons. Even though the web buckling of prismatic and tapered I-beams behavior was widely investigated in literature, the behavior of stepped beams with depth discontinuity remains largely unexplored. This paper aims to provide a comprehensive analysis of web buckling in steel stepped I girders and beams and recommend different options for dealing with such a problem.

LITERATURE REVIEW

Barrau et al. [1] studied the post-buckling of a stiffened beam subjected to a single shear load. They used Wagner's theory and a non-linear finite element method to analyse the problem. A new approach was suggested to investigate post-buckling behaviour, where two zones are assumed in each panel, an inner zone with a damage law and an outside zone containing the original material. The outcomes of this analysis were in good agreement with the findings of the experiments. Loaiza et al. [2] proposed an approach for evaluating the effect of longitudinal stiffening of plate girder webs subjected to concentrated loads on the ultimate strength. The approach is based on a plastic collapse mechanism. The stiffener's influence is then accounted for in a closed-form solution. Theoretical predictions match well with the available experimental results. Shi and Xu [3] conducted experiments on Q550 high-strength steel I-section beams under moment gradient (MG) and under patch loading (PL), to investigate the local buckling behaviour. The specimens' failure modes, critical local buckling strengths, ultimate strengths, load–deformation curves, load–strain curves, and moment–rotation curves were obtained. The test data were compared with the design results by ANSI/AISC 360-16, Eurocode 3, AS 4100-1998, AIJ LSD 2010, and GB 50017-2003. Nascimento et al. [4] showed that the formula for the web slenderness limit given in EN 1993-1-5 to prevent flange-induced buckling applied to S690 high-strength steel (HSS) plate girders provides lower slenderness limits, expected to govern web design and limit potential for reducing their thickness to benefit from the high steel strength. The authors analysed the formula and compared the web slenderness limitations to numerical results from a non-linear analysis of such girders. Ragheb [5] reported an analytical investigation of the impact of flange–web interaction on local buckling of welded steel I-sections. A proposed inelastic local buckling stability model considers the geometric and material characteristics. The deformation theory of plasticity explained steel's behaviour beyond the elastic limit. The model's outputs were compared with published experimental data and results from the finite element analysis. New width-to-thickness limits that consider all of the section's properties were suggested.

Couto and Real [6] examined the interaction of local buckling with the global lateral-torsional buckling of I-shaped girders with slender sections. Using material and geometrical nonlinear finite element analysis, the authors investigated the impact of residual stresses and geometrical imperfections on such elements. The results were compared to the American AISC360-16 design code and European Eurocode 3. AISC360-16 gave an upper limit for the beam's resistance. Still, Eurocode 3 provided a lower limit, owing to the considerable impact of residual stresses on the carrying capacity of beams with slender sections. Sener et al. [7] outlined an experimental and numerical study of steel beams' web compression buckling strength subjected to concentric loads distributed over lengths greater than the member depth. The study includes experimental testing to assess the effects of load width on buckling strength under sustained loading, with load widths approximately 2.5 times larger than the section depth. The experimental data were utilized to assess numerical finite element simulations, which considered the impact of geometric defects, residual stresses, and material inelasticity. Mamazizi et al. [8] study encompasses two experimental tests, considering both rigid and non-rigid end posts. The data obtained were utilized to validate the numerical modelling. In addition, the post-buckling capacity was compared with the current specification codes. The findings indicate an intense match between the codes and numerical analysis when the web slenderness is between 120 and 220. Nonetheless, a significant divergence is observed in the results when the web slenderness falls outside this range.

Witte [9] conducted an experimental and numerical study of web compression buckling in steel I-section beams. Experimental tests were conducted on specimens with load widths of approximately 2.5, 1.75, and 1.5 times their section depth. Creep effects were also investigated. Test results were utilized to calibrate the numerical modelling. Topkaya [10] assessed the sidesway web buckling equations used by the AISC-LRFD specification. A finite element analysis is used to identify the parameters that influence the web buckling of supported beams subjected to concentrated loads. A new set of design equations was proposed by combining the results of the numerical study with the fundamentals of plate buckling theory. A lateral buckling type of instability, preceding sidesway web buckling, has been identified for beams with negative end moments. Sediek et al. [11] studied the ultimate shear strength of tapered imperfect end web panels in steel plate girders. Using numerical modeling, the effect of initial geometric imperfections on the ultimate and post-buckling shear strengths was investigated.

Ammash and Shaffaf [12] numerically investigated web shear buckling failure of flat web specimens and webs with honeycomb patterns. The shear buckling resistance of the honeycomb web plate girder was significantly higher than that of the flat web. Abbas [13] studied the behaviour of steel I-section beams with web openings. An experimental and nonlinear numerical analysis was conducted on six steel I-beams with different opening shapes, such as circular, rectangular, and hexagonal. The beam with a circular opening was stronger than a rectangular opening beam. Also, the beam with hexagonal openings was stronger than that with rectangular openings. Al-Mazini [14] investigated the structural behaviour of steel plate girders with circular and square web openings experimentally and numerically, under two-point loads. The results showed that the ultimate load capacity of the girders decreases with increasing opening size, and the position of the plastic hinge depends on the size of the hole. Another study by El-Dehemy [15] analysed steel beams with different web opening configurations using nonlinear static and dynamic analysis. Hamed [16] used the finite element method to study the critical shear buckling of tapered plate girders containing a circular or square opening. The analysis considered the effects of tapering angle and hole size on the average height of the web, aspect ratio, depth-to-thickness ratio, and the boundary conditions between the web and flanges.

Niu et al. [17] presents an experimental program examining the buckling of stainless steel I-section beams due to local–global interactions. Austenitic S30401, ferritic S44330, and lean duplex S32101 alloys were studied. Six laterally braced tests and twenty-four unbraced tests with spans varying from 1.9 to 4.0 m comprised the test program. In the testing, interaction buckling was successfully captured.

Most recent research in the literature investigates steel beams with a non-uniform section along their length. Park and Stallings [18] investigated stepped beams' Lateral Torsional Buckling (LTB) capacity, where straightforward design formulas were suggested. Using the finite element method, Surla et al. [19] studied the inelastic buckling capacity of unsymmetric stepped I-beams under uniform bending. The considered stepped beams had non-compact flanges and a wide range of asymmetry about the x-axis. Both doubly and singly stepped beams were studied, and the results were compared with different design standards. Alolod et al. [20] evaluated the applicability of the stepped beam factors for the stepped I-beams' LTB capacities at their midspans, subjected to high temperatures. A series of numerical investigations evaluated the buckling behavior of stepped beams, which was carried out using the finite element analysis, where heat transfer was also considered. Reichenbach et al. [21] proposed simplified formulas that calculate the buckling capacity of stepped steel beams. This parametric study, which included prismatic and non-prismatic beam sections, investigated the effects of common span-to-depth ratios, intermediate bracing schemes, degrees of mono-symmetry, variable flange transitions, and moment gradients on the buckling response.

All the aforementioned research considered stepping as changes in flange thickness and width, but none investigated the change in the beam total depth. The only research that could be found studying sudden depth changing beams is by Trinh et al. [22] and Almasri and Jabur [23], where they studied lateral torsional buckling behavior. No one reference could be found investigating the local web buckling of stepped girders. To cover a gap in this topic, the current study will present a case study of a web local buckling failure of steel girders, and investigate web buckling behavior of steel girders with abrupt stepped depth under different conditions.

METHODOLOGY

To study the web buckling of the stepped steel girders, linear finite element eigenvalue buckling analysis is utilized here through the finite element software Mecway 16 [24], which is based on the open-source finite element solver CalculiX. The study includes three parts. The first part is a verification of the finite element analysis of prismatic steel girders without varying depths, which will be compared with experimental data from literature in addition to a comparison with design codes and standards, namely the AISC360-16 [25] and Eurocode 3 EN 1993-1-5 [26]. The second part will discuss a failure case study where steel girders with stepped I-section girders suffered web buckling during construction. The third part will investigate the effect of different parameters on the web buckling of stepped steel girders, namely, step height, step location, boundary conditions, and adding stiffeners.

VERIFICATION

In order to verify the use of the linear eigenvalue finite element method in studying the web buckling of steel girders, the results of the experiments by Holtz and Kulak [27] were used. They tested two non-compact beams subjected to strong-axis bending, WS-12-N and WS-13-N. The specimens were fabricated from CSA G40.12 plate, with a yield strength of 303 MPa (44 ksi). The steel modulus of elasticity and Poisson's ratio are 200,000 MPa and 0.3, respectively. No information was available about residual stresses. The beam specimens were supported and loaded symmetrically with two equal concentrated loads acting on tension flanges, so a uniform moment region existed in the middle of the beams. The beams' spans were 4876.8 mm (192 in) and 5486.4 mm (216 in), with the two loads being at 1981.2 mm (78 in) and 2286 mm (90 in) from the supports. The beams were laterally braced at the load and reaction points to prevent lateral movement. The flanges were 279.4 mm (11 in) by 9.525 mm (0.375 in). The web's thickness was 6.35 mm (0.25 in), and clear heights between flanges were 683.26 mm (27 in) and 736.6 mm (29 in). A Quad4 shell element was used for the simulation purposes. Quad elements are more accurate than triangular elements, and more suitable for the research problem with straight geometries. The Quad8 element was tried, and the same accuracy was obtained as the Quad4 element. So, the Quad4 shell element was considered suitable for the current research problem. The element avoids shear locking as well as membrane locking. It is suitable for simulating thin structures such as the steel I girders. Each node has 6 degrees of freedom; displacement in X, Y, and Z, and rotation about X, Y, and Z. Uniform meshing is used throughout the girders. The concentrated loads usually cause stresses concentration in the static finite element load-deformation analysis. Refined mesh with smaller element size is usually used to enhance the accuracy of the results in this case. However, for the linear eigenvalue buckling analysis, which is a stability analysis, it was found that the results are reasonably accurate, without using very fine meshes, as will be shown later, as the buckling analysis finds the loads at which a structure's stiffness matrix becomes singular, meaning it loses its ability to resist further deformation. Refining the mesh around the critical areas did not significantly improve the accuracy of the buckling capacity. Therefore, meshes were kept uniform for the rest of the study. A convergence check of the finite element buckling moment results of the WS-12-N specimen was carried out and illustrated in Fig. 2. The curve shows that using around 20 thousand nodes obtains satisfactory accuracy and therefore can be considered an appropriate mesh size.

Next, the two beam samples were modelled, and buckling moments were obtained. Fig. 3a shows the loading and boundary conditions of the WS-12-N beam. It is supported at the edge of the lower flange, where translations in three directions are restrained along the edge, and subjected to two-point concentrated loads. Fig. 3b shows the web buckling of the beam at the loading position, which was the first predicted buckling mode. Buckling displacement of about 0.76 mm matches the one in Holtz and Kulak [27], which was about 0.8 mm

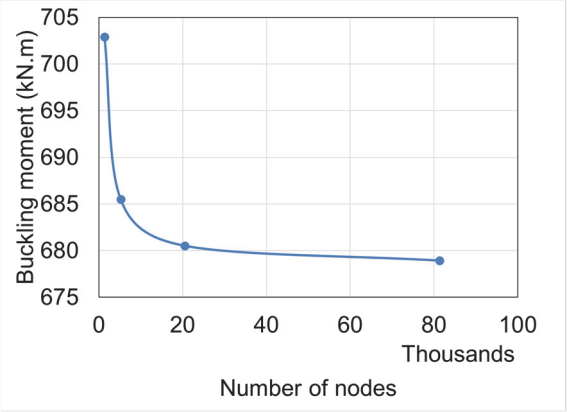

Figure 2: Convergence of finite element modeling of WS-12-N specimen.

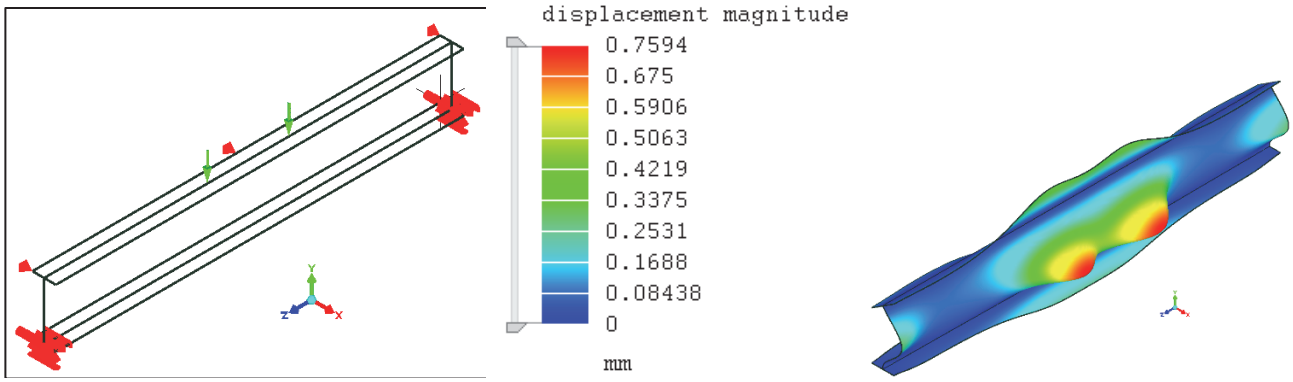

(a) (b)

Figure 3: (a) loading and boundary conditions of WS-12-N specimen, and (b) first buckling mode of WS-12-N specimen.

Buckling moments simulation results are illustrated in Fig. 4, along with the experimental values, and values calculated by AISC-360 specifications [25] and Eurocode 3 [26]. The web buckling strength R_n calculated by AISC-360 (which calls it web crippling) is obtained by the equation (in British units):

$$R_n = 0.80 t_w^2 \left[1 + 3\left(\frac{l_b}{d}\right)\left(\frac{t_w}{t_f}\right)^{1.5} \right] \sqrt{\frac{E F_{yw} t_f}{t_w}} \tag{1}$$

where t_w is web thickness, t_f is flange thickness, d is the full depth of the member, l_b is the length of bearing, E is the modulus of elasticity, and F_{yw} is the specified minimum yield stress of the web. As the load in the experiment was applied to the tension flange, the length of the bearing is assumed to be zero here. It should be noted that by setting the bearing length to zero, the value obtained by Eqn. (1) becomes independent of web height. So, the calculated web buckling load will be the same for the two samples. However, the buckling moment will differ for the two specimens due to the difference in span and loading position. For the Eurocode 3, design resistance to local buckling under transverse force should be calculated from:

$$F_{Rd} = \frac{F_{yw} L_{eff} t_w}{\gamma_{M1}} \tag{2}$$

where L_{eff} is the effective length for resistance to transverse forces, and γ_{M1} is a safety factor, taken as 1 here. A good agreement is noticed between experimental and numerical buckling moments for the girders. As shown in Fig. 4, the

buckling moments obtained by the finite element method for the two samples were 681 and 702, around 12% and 9% higher than the experimental results. The finite element analysis was linear, with no consideration for residual stresses or initial imperfections, so the simulation is considered acceptable for such a problem. The AISC-360 formula results in a buckling moment of 610 kN.m for the WS-12-N sample, which is very close to the experimental result. However, it calculated the buckling moment to be 703 kN.m for the WS-13-N sample, which is about 9% higher than the experimental result, coinciding with the finite element method result. Conversely, the Eurocode 3 underestimated the buckling moments of the two samples considerably, at 439 kN.m and 500 kN.m, which is about 72% and 78% of the experimental strength, respectively.

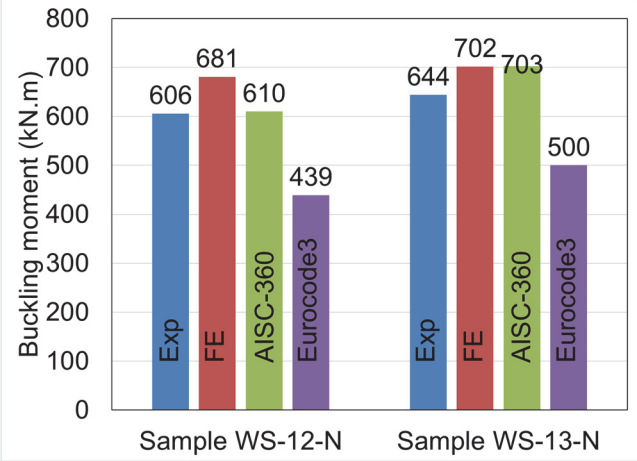

Figure 4: Comparison of buckling moment values.

CASE STUDY

On July 12, 2023, a failure incident occurred on the Albany County Rail Trail's new bridge in Slingerlands, New York [28]. The original bridge, shown in Fig. 5a, was old and struck multiple times by vehicles and was scheduled to be replaced with a new, higher clearance one, shown in Fig. 5b. The new steel bridge girders buckled during construction. The sudden deformation in the girders occurred during the casting of the concrete decking. The steel began to hinge, and the girders collapsed in on themselves and then downward until they came to rest on the retaining walls, where complete collapse was stopped, as shown in Fig. 5c. Fortunately, no casualties were reported.

(a) (b)

(c)

Figure 5: (a) the old replaced bridge, (b) the new girder before installation, and (c) the new bridge showing the buckled zone during construction.

According to a report Albany County commissioned [29], a design flaw led to the buckling of the bridge girders. The old bridge was constructed with three separate spans, with the middle span being deeper than the two neighboring spans, as shown in Fig. 5a. The new bridge was designed to mimic the old bridge, so each of the two girders that supported the bridge's span had two locations where the top flange of the girder transitioned from deeper to shallower sections. That transition was abrupt, in a "step" configuration from horizontal to vertical. This type of girder transition in depth is usually performed gradually over a longer length, and not abruptly as a step. Such a step resulted in a concentration of stress in the girder's web. In addition, unlike the original bridge design, the new bridge design did not include a support under this abrupt section transition. It did not appear that the construction means and methods were the cause of the collapse.

The girder section is shown in Fig. 5b. The new bridge's total span is about 41.9 m, with the middle deeper section length of about 21 m. The bridge width is about 4.5 m. The deeper section depth is about 1630 mm, while the shallower section depth is about 1085 mm, estimated from the figures' scaling. It means that the shallower section depth is about two-thirds of the deeper section depth. The flange thickness is about 43 mm, and the web thickness is about 10 mm. The steel grade is unknown, so it is assumed to be either F_y = 250 MPa or F_y = 350 MPa grade. This means that the slenderness ratio for the deeper and shallower sections of the web is about 154 and 100, respectively. This is classified as slender (class 4) for deeper section web, and semi-compact (class 3) for shallower section web, according to Eurocode 3. However, according to AISC360-16 standards, the deeper section web is considered slender if F_y was 350 MPa and noncompact if F_y was 250 MPa, while the shallower section web is noncompact if F_y = 350 MPa and compact if F_y = 250 MPa. It is illustrated in Tab. 1. These estimations show significant differences in different codes when classifying steel elements.

section	h (mm)	t_w (mm)	h/t_w	AISC360		Eurocode 3	
				$F_y = 250MPa$	$F_y = 350MPa$	$F_y = 250MPa$	$F_y = 350MPa$
Deeper section	1544	10	154	noncompact	slender	class 4 Slender	class 4 slender
Shallower section	999	10	100	compact	noncompact	class 3 Semi-compact	class 3 Semi-compact

Table 1: Classification of deeper and shallower webs of girders.

The steel girder is simulated using the linear finite element method to find the linear eigenvalues and buckling failure load. The girders were supported on the abutments. Stiffeners with a thickness equal to the web thickness were used. Lateral supports at the lower part of the web were implemented to simulate the effect of the steel diaphragms used in the bridge. Distributed load per length was applied to the face of the bottom flange, simulating the weight of the slab deck. As the buckling happened during concrete casting, half of the concrete deck is assumed to be applied as a load on the steel girder. The web buckling at the section step was the first buckling mode, illustrated in Fig. 6, with the buckling failure load being

about 15.6 kN/m. Assuming the concrete deck was about 25 cm thick, with a deck width of about 4.5 m, the weight of the concrete deck on every girder that caused the buckling will be around 14.1 kN/m. It shows that the finite element analysis can be considered very acceptable in evaluating the buckling strength of the web at this abrupt change in the section depth. Buckling analysis of complex steel geometries should be mandatory, just like the static analysis, to avoid failure cases. The finite element method will be used next to study the effect of different parameters on such a problem.

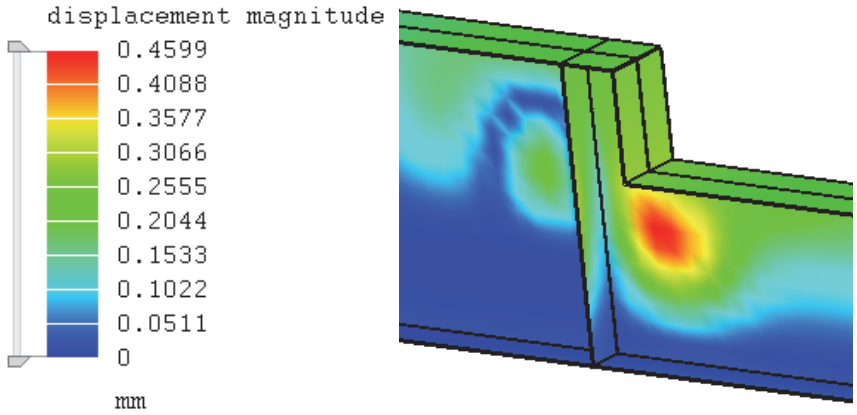

Figure 6: Web buckling simulation of the failed steel girder.

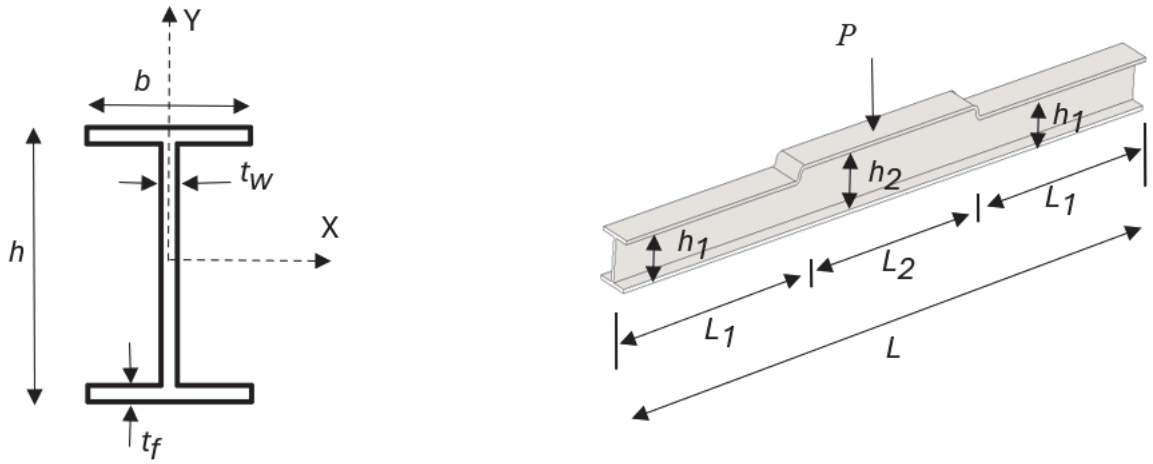

Figure 7: Girder geometry and dimensions.

PARAMETRIC STUDY

Different parameters can affect stepped steel girders' web buckling strength and behavior. The parameters studied in this research are step height, step location, boundary conditions, and adding stiffeners. The geometry of the simulated girders is illustrated in Fig. 7. The steel modulus of elasticity and Poisson's ratio are 200,000 MPa and 0.3, respectively. The yield strength of steel was taken as 350 MPa. The girder is assumed to be supported, where the edge of the bottom flange is restrained from movement in the three directions, as shown in Fig. 3a. The girder is subjected to one concentrated load at the middle of the girder span. It should be noted that elastic buckling was assumed throughout the analysis. The buckling load was very low, so no plastic stresses were reached, neither at the step nor the boundaries nor the applied load. The corners were made without filleting, as filleting showed an insignificant effect on the results. The mesh sensitivity of a stepped beam was investigated and illustrated in Fig. 8. The convergence of the buckling load with the number of nodes was seen to be faster than the convergence of the maximum Von Mises stress near the step. Around 100,000 nodes was enough to get good accuracy for the buckling load, while for the same problem about 500,000 nodes was not enough to achieve acceptable accuracy for the Von Mises stress. Although the buckling eigenvalue analysis depends initially on the static linear analysis, its sensitivity to mesh size was seen to be considerably lower. This can be attributed to the fact that linear static analysis is concerned with local stress and strain values that can change dramatically

over small distances, so a fine mesh is necessary to capture their sharp gradients. Buckling on the other side is more of a global phenomena, not related only to a specific point or node. It is a macro-scale deformation pattern that affect the entire structure, or at least a large part of it. The buckling calculation is looking for a condition where the entire system's stiffness is zero. This global scale matrix operation is less sensitive to small variations in the individual element stiffnesses than a linear static analysis is to local stress gradients.

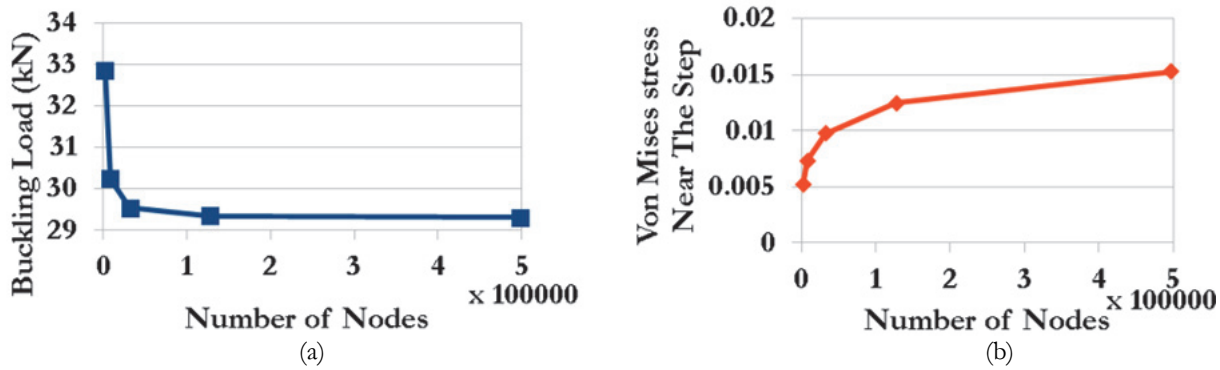

Figure 8: Mesh sensitivity of stepped beam with h_1 =400mm, h_2 =800mm, L_1 =3m for (a) buckling load, and (b) maximum Von Mises stress near the step.

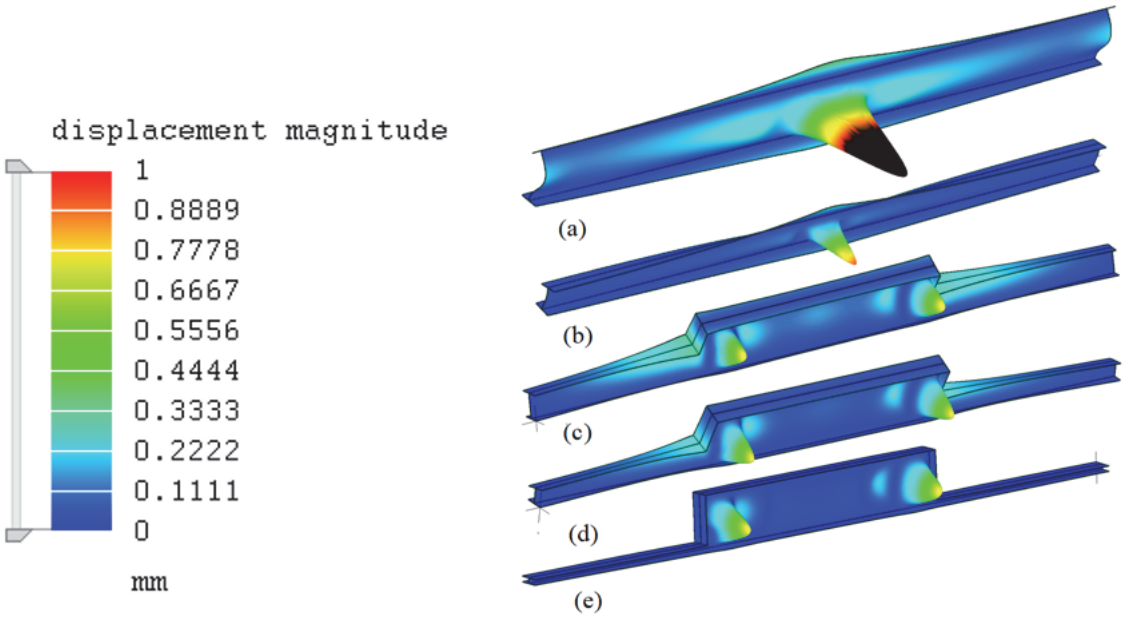

Figure 9: Web buckling for prismatic girders (a) h = 800 mm, (b) h = 400 mm, and stepped girders (c) h_1 = 400 mm, h_2 = 800 mm, (d) h_1 = 240 mm, h_2 = 800 mm, and (e) h_1 = 80 mm, h_2 = 800 mm. All girders have the same deformation scale factor = 1000.

Step height

A supported girder under one concentrated load at the middle of the girder is considered for the study of the effect of step height. At first, prismatic girders with h = 400 and 800 mm depth were modelled, with b = 300 mm, t_w = 4 mm, t_f = 16 mm, and a span of 10 m. The girders are laterally supported at the ends and in the middle of the top flange. Then, stepped girders with h_2 = 800 mm, h_1 = 400, 240, and 80 mm, L_1 = 3 m, and L_2 = 4 m were simulated. The first buckling mode shapes are illustrated in Fig. 9 for the five cases. The buckling load for the prismatic girders with 400 and 800 mm height was 154.62 kN and 73.15 kN, respectively. The larger height leads to a lower web buckling load. However, when a step is proposed to the section depth, the local web buckling happens at the step location on the deeper section side, rather than under the concentrated load at the middle of the girder. In addition, the web buckling loads were 29.65,

25.25 and 29.30 kN for h_1 = 400, 240 and 80 mm girders, respectively. The web buckling capacity is not highly dependent on step height and is considerably below the local web buckling capacity of the prismatic girder. The step causes a discontinuity in the top flange, disrupting its ability to transfer compressive stress. Some of this compressive stress is transferred through the web, which causes the web to buckle at the step location. However, there is no external load there. These compressive stresses are related mainly to the applied load and the girder span, so if the girder span is decreased, the web buckling capacity at the step is expected to increase.

The buckling load versus step depth is plotted in Fig. 10 for girders with different practical h_2 depths, namely 1000, 800, and 600 mm. The figure shows values for two buckling modes; one buckling occurs under the applied concentrated load at the middle of the girder, and the other at the step. The lower value buckling is the first buckling mode, while the other is the higher one. When h_1 / h_2 = 0.9 (10% step), the first buckling mode was the buckling at the load location. However, when the step is higher than this, the buckling at the step becomes dominant. The buckling strength reduces quickly as the step increases to about 50% of the section depth. After that, increasing the step will barely affect the buckling load. The curve of the buckling at the load showed a drop in value at some of the step thicknesses due to some interaction between the buckling of the two locations. The buckling capacity reduction reached about 73% (from around 100 kN to around 27 kN) for the case of h_1 / h_2 = 0.3 and h_2 = 600mm.

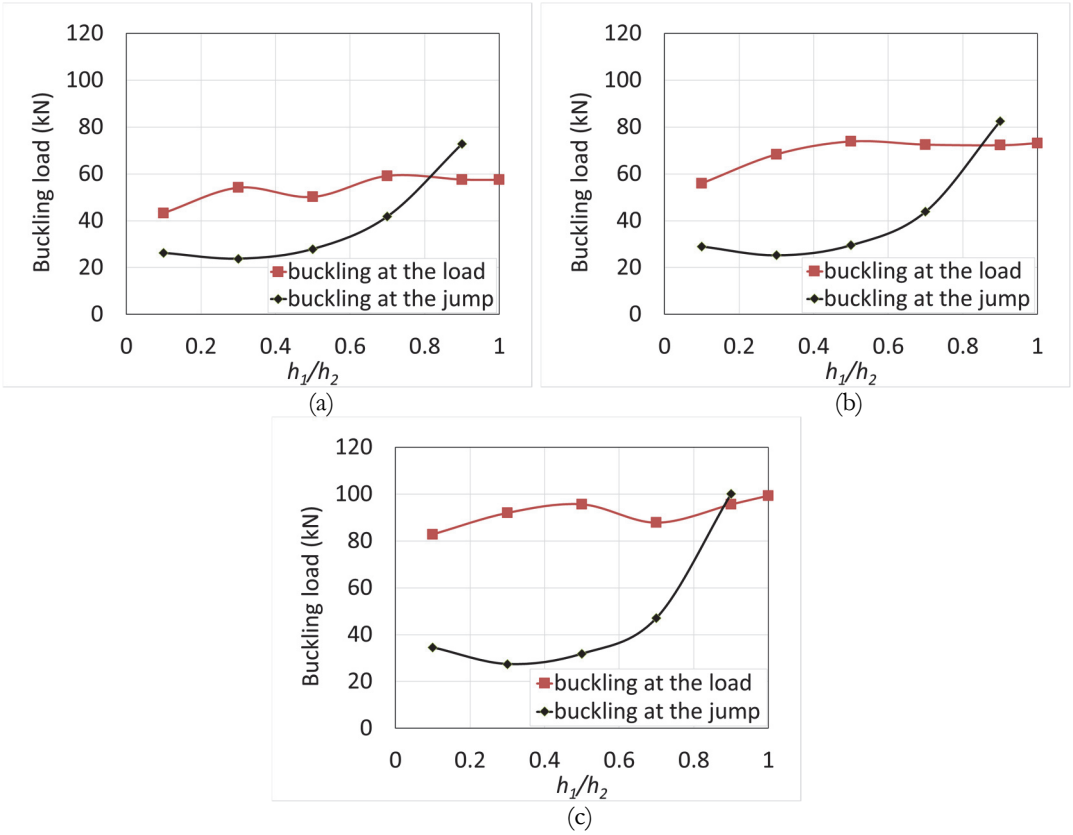

Figure 10: Buckling load versus step depth considering buckling either at the applied load (middle of the girder) or at the step, for (a) h_2 = 1000 mm, (b) h_2 = 800 mm, and (c) h_2 = 600 mm.

Step location

The buckling behavior of the girder was modeled for girders with the section step being at the top compression flange and once again at the bottom tension flange of a supported girder. The girder is subjected to one concentrated load at the middle of the top flange. The girder has dimensions b = 300 mm, t_w = 4 mm, t_f = 16 mm, h_1 = 400 mm, h_2 = 800 mm, span of 10 m, L_1 = 3 m, and L_2 = 4 m. The girder is laterally supported at the ends and in the middle of the top flange. The first buckling mode shapes of stepped girders are illustrated in Fig. 11, along with the results of the prismatic girders. The girder with the step made in the lower flange showed local buckling at the applied load location rather than at

the step location, with a buckling strength of 67.65 kN. It is close to the value of the prismatic girder with h = 800 mm, which was 73.15 kN, which indicates that the step effect is limited when it is in the tension flange.

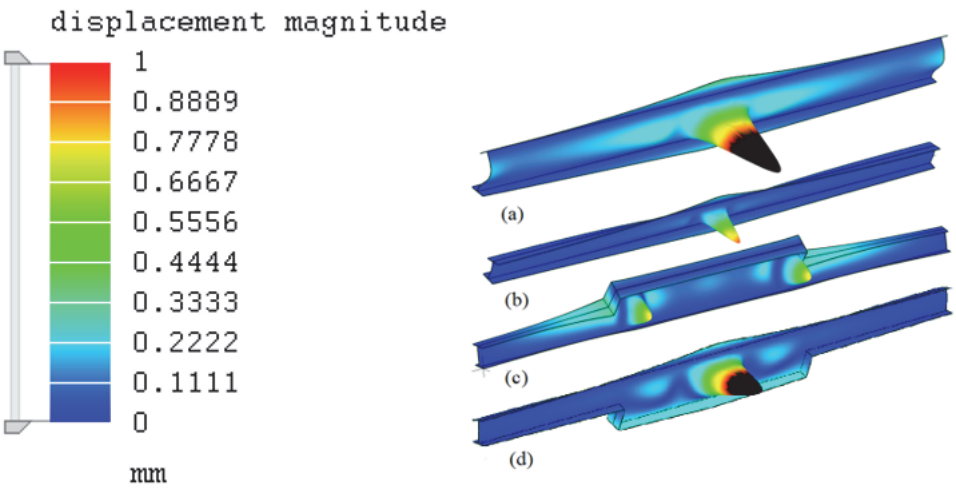

Figure 11: Web buckling for prismatic girders (a) h = 800 mm, (b) h = 400 mm, and stepped girders (c) h_1 = 400 mm, h_2 = 800 mm, step at the top flange, and (d) h_1 = 240 mm, h_2 = 800 mm, step at the bottom flange. All girders have the same deformation scale factor = 1000.

Boundary conditions

The effect of two boundary condition types is investigated here: simply supporting and fixed supporting boundary conditions. For the supported case, the edge of the bottom flange was restrained from movement in the three directions, similar to Fig. 3a. On the other hand, for the fixed-supported case, all the nodes at the girder's ends (at the flanges and the web) were restrained against translations and rotations. The modeled girder has dimensions h = 300 mm, t_w = 4 mm, t_f = 16 mm, h_2 = 800 mm, and a span of 10 m. Different step height values h_1 = 800 (prismatic girder), 720, 560, 400, 240, and 80 mm, with L_1 = 3 m, and L_2 = 4 m were simulated. The girder is laterally supported at the ends and in the middle of the top flange. The effect of simple versus fixed support on the buckling load capacity of the stepped girder at different step heights is shown in Fig. 12. When the girder is prismatic with no step, the buckling load increased from 73.15 kN for simple support to 85.36 kN for fixed support, which is about a 14.3% difference, and the web buckling occurred under the load at the middle of the girder. The fixation of the girder reduces the moment at the girder middle to half, which also reduces the compressive stresses above the neutral axis to half. It could indicate that the compressive stress above the neutral axis contributes to the web buckling load capacity. The compressive stress parallel to the girder span is perpendicular to the compressive stress from the applied transverse load, which forms a biaxial stress state. The web buckling capacity formulae in AISC-360 and Eurocode 3 are unrelated to the bending moment or the compressive stresses at the buckling location. At the same time, it appears to be a significant factor. When introducing the step to the web of the girder, web buckling capacity remained almost the same up to a step of 15% of section depth (h_1 / h_2 = 0.85) for simple support and 60% of section depth (h_1 / h_2 = 0.4) for fixed support, where web buckling remained to occur at the load location. After these values, web buckling at the step becomes dominant as the first buckling mode, where buckling capacity decreases significantly to reach eventually around 40% of the original girder capacity for the case of simple support. However, the reduction reaches only about 10% for the case of fixed support. It can be partly attributed to the fact that the step in the fixed girder is about 0.5 m away from the theoretical inflection point in the moment diagram, which has zero moment, so longitudinal stresses are expected to be significantly lower when compared with the supported girder. Fixation of the girder ends greatly helps counteract the degrading effect of the girder web stepping.

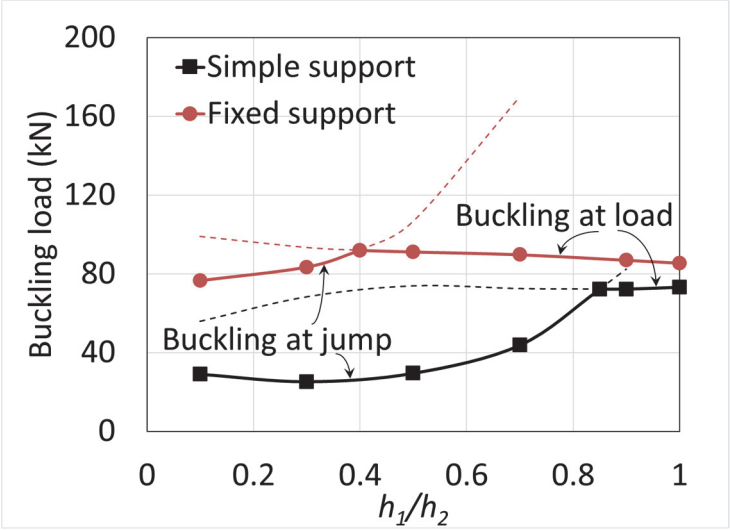

Figure 12: Comparison of the effect of simple versus fixed support on the buckling load of the stepped girder.

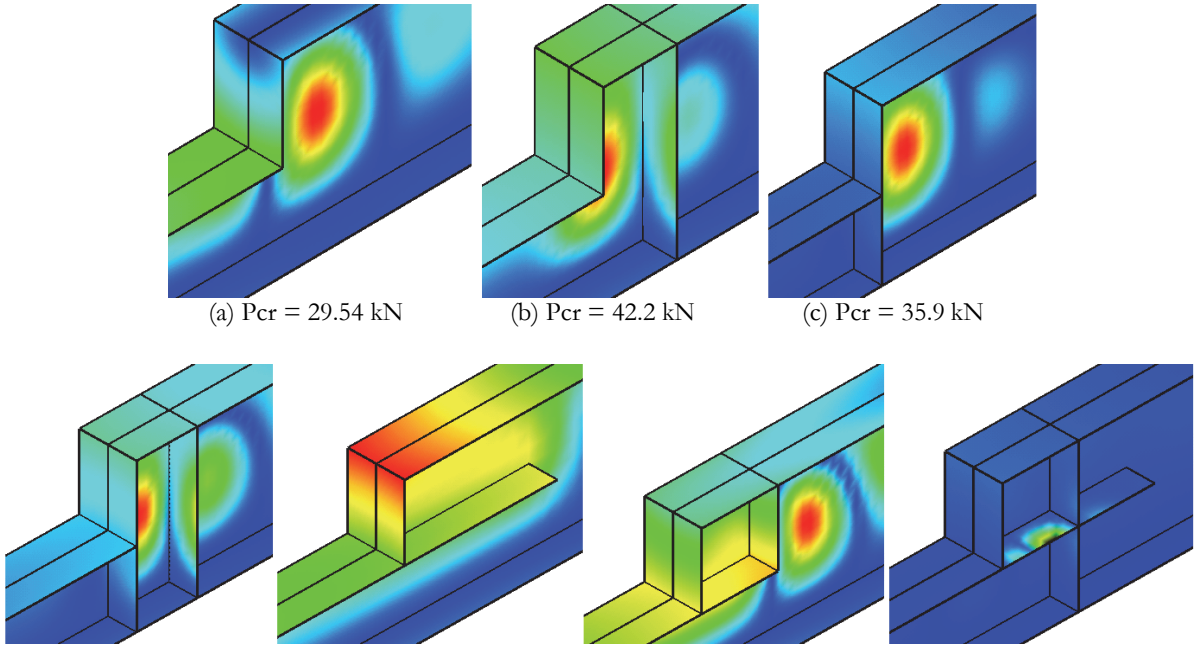

(a) Pcr = 29.54 kN (b) Pcr = 42.2 kN (c) Pcr = 35.9 kN

(d) Pcr = 50 kN (e) Pcr = 74 kN (f) Pcr = 66.9 kN (g) Pcr = 161.8 kN

Figure 13: Buckling shape and load at the section step for the different stiffeners configurations, (a) no stiffeners (NS), (b) long vertical stiffener (V_1), (c) short vertical stiffener (V_2), (d) long and short vertical stiffeners (V_3), (e) long horizontal stiffener (H_1), (f) short vertical and horizontal stiffeners (VH_1), and (g) long vertical and horizontal stiffeners (VH_2).

Stiffeners

Six different stiffener configurations are modeled to study their effect on the local web buckling at the web section step. Three configurations included vertical stiffeners (named V_1, V_2, and V_3), one included a horizontal stiffener (named H_1), and two included both vertical and horizontal stiffeners (named VH_1 and VH_2), as shown in Fig. 13. They were modeled and compared with a section step with no stiffener (NS). All stiffeners have a thickness equal to the web thickness. The girder has dimensions h_2 = 800 mm, h_1 = 400, b = 300 mm, t_w = 4 mm, t_f = 16 mm, L_1 = 3 m, L_2 = 4 m, and span of 10 m. The girders are laterally supported at the ends and in the middle of the top flange to avoid any lateral torsional buckling. The stiffeners were assumed to be fully welded to the web and flanges of the girders. No contact interaction was used in the finite element analysis. The stiffeners' welding was not investigated in this research, and was assumed to have enough strength to keep the stiffeners working fully with the girder. The simulation buckling analysis

results are plotted in Fig. 13. As obtained earlier, the buckling load for the case with no stiffeners was 29.54 kN. When a long vertical stiffener is used at a distance from the step equal to the step height, the buckling load increases to about 42.2 kN, which is about 43% more. When a short vertical stiffener is used exactly below the step, the buckling load increases to about 35.9 kN, only about 22% more. However, using long and short vertical stiffeners increased the buckling load to 50 kN, which is about 69% more strength, indicating an interaction effect between stiffeners. On the other hand, using a horizontal stiffener with a length equal to the web height has increased the web buckling capacity to about 74 kN, which is very close to the web buckling capacity under the applied concentrated load. In this case, there was no clear web buckling, but rather a flange-web buckling interaction. It also agrees with the previous discussion that the longitudinal compressive stresses mainly influence the local web buckling at the step in the flange and web. Hence, the horizontal stiffener was more successful in restoring the buckling capacity of the web. When short vertical and horizontal stiffeners were used, the buckling load increased to 66.9 kN. It is higher than the case of the two vertical stiffeners, but lower than that of a long horizontal stiffener. The final configuration with long horizontal and vertical stiffeners prevented the local buckling at the web. It showed only buckling in the horizontal stiffener at a load of 161.8 kN, much more than the first buckling mode at the applied load location.

Static analysis

To ensure that the linear buckling analysis is valid, linear static analysis was conducted to the previously analyzed cases to ensure the stresses did not reach the yielding stress. The axial stress along the beam axis is shown in Fig. 14 for a sample supported girder with h_1 = 400 mm, h_2 = 800 mm, and L_1 = 3 m. The buckling load was 29.6 kN. The stress is transferred from the top part of the upper compression flange to the lower part of the compression flange through the web. This horizontal compressive stress was the leading cause of the buckling at that area, and that's why the horizontal stiffener was more effective in resisting the possibility. Yet, axial stress of around 302 MPa did not reach the assumed yielding stress of 350 MPa, so linear buckling analysis is believed to be valid. Although stress concentration was noticed in the static analysis, its effect was not as significant in the eigenvalue buckling analysis, as was shown before. Nonlinear buckling analysis was also conducted to check if the linear buckling analysis was valid or not. Bilinear stress strain is used here with tangent modulus being 4.5 GPa, with a concentrated load of 60 kN, shifted 1 mm from the top flange center to represent geometrical imperfection, as a perfectly symmetric model won't buckle in nonlinear analysis. The nonlinear analysis predicted the buckling load to be about 32 kN, which is 7.5% higher than the eigenvalue analysis. Black colored stress indicating stress beyond yield point only appeared after the onset of the buckling, indicating that linear buckling analysis is valid to estimate the buckling load.

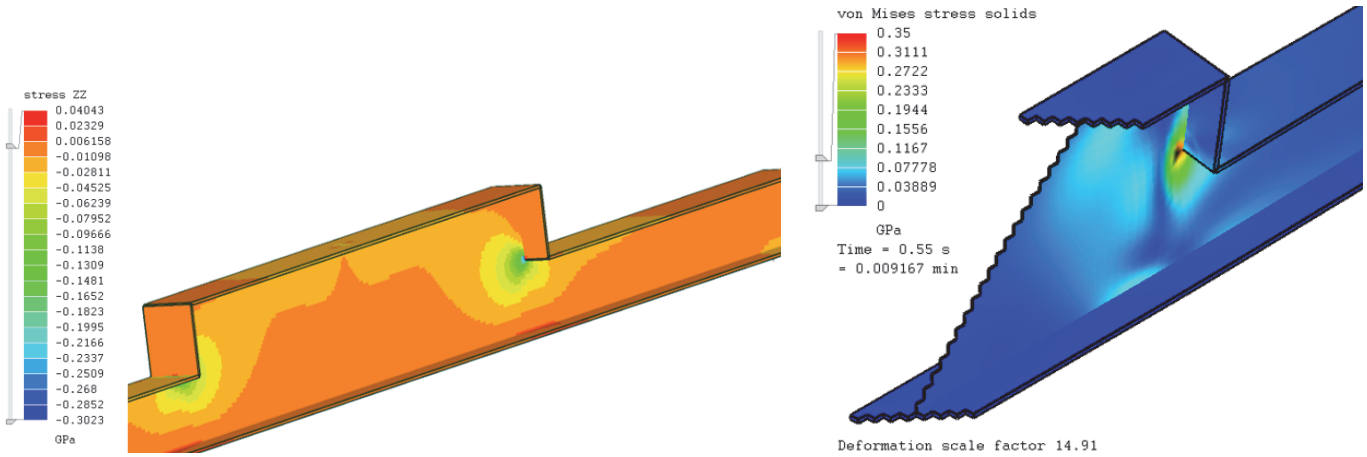

(a) (b)

Figure 14: (a) Axial stress along a girder sample in linear static analysis, and (b) nonlinear von Mises stress after buckling started.

Limitations

Although the current study investigated the effect of different parameters on a stepped steel I girder's web buckling, several limitations arise here. For example, various buckling modes interaction could occur for some geometries, where no clear buckling can be identified. It was noticed that when a horizontal stiffener was used, the flange and web buckled as a single unit. Also, assuming supported or fixed supported girders idealizes the real-world situation. If the girder is part of a

frame or supported by a column, the results would differ from those obtained here. Hence, it is advised to simulate every case with its unique conditions.

Conclusions

In this paper, the local web buckling of stepped steel I-section girders was studied. Firstly, linear eigenvalue buckling finite element analysis showed an excellent and acceptable accuracy in simulating complex local buckling cases with an overestimation of roughly 10% of buckling capacity compared with experimental results. On the other hand, codes can vary significantly in estimating the web local buckling in steel girders. Hence, using the finite element method can be very helpful in solving such complex problems. Buckling analysis of complex steel geometries using the finite element method may be mandated to avoid any possible buckling failure. Proposing a step in the steel I-section girders' compressive flange disturbs the stress continuity in the flange. It puts high local horizontal compressive stress on the web, leading to local buckling at the step. Large stepping of a steel girder degrades the girder's capacity significantly. Different actions are possible to mitigate the effects of the stepping. Moving the step from the compression flange to the tension flange can help significantly restore the web buckling capacity. If the stepping was necessary to be in the compression flange, moving it from a higher moment point to a lower moment point can also help the web to support higher loads. Another option is to use stiffeners to resist the possible web buckling. Horizontal stiffener showed higher resistance to web local buckling at the step than the vertical stiffener. In the end, stability buckling analysis was seen to be less sensitive to numerical singularities than traditional static analysis. The effect of such numerical singularities on buckling analysis is recommended to be studied in the future.

Credit authorship contribution statement

Amin H. Almasri: Investigation, Formal analysis, Validation, Supervision, Project administration, Methodology, Conceptualization, Visualization, Writing – review & editing, Writing – original draft.
Mohammad Nadeem Akhtar: Visualization, Writing – review & editing, Writing – original draft.

Declaration of competing interest

The authors declare that they have no known competing financial interests or personal relationships that could have appeared to influence the work reported in this paper.

Data availability

Data will be made available on request.

References

[1] Barrau, J.-J., Creze, S., Castanie, B. (2005). Buckling and post-buckling of beams with flat webs. Thin-Walled Structures 43, 877–894. DOI: https://doi.org/10.1016/j.tws.2005.01.001.
[2] Loaiza, N., Graciano, C., Chacón, R. (2018). Web Crippling Strength of Longitudinally Stiffened Steel Plate Girder Webs Subjected to Concentrated Loading. Eng J 55, pp. 191–201. DOI: https://doi.org/10.62913/engj.v55i3.1133.
[3] Shi, Y., Xu, K. (2019). Experimental and Analytical Study on Local Buckling Behavior of High Strength Steel Welded I-Section Beams. Int J Steel Struct 19, pp. 1171–1190. DOI: https://doi.org/10.1007/s13296-018-0196-6.

[4] Nascimento, S., Pedro, J.J.O., Biscaya, A. (2020). Web buckling of high-strength steel plate girders induced by bending curvature. Steel Construction 13, pp. 84–91. DOI: https://doi.org/10.1002/stco.202000015.
[5] Ragheb, W.F. (2015). Local buckling of welded steel I-beams considering flange–web interaction. Thin-Walled Structures 97, pp. 241–249. DOI: https://doi.org/10.1016/j.tws.2015.09.026.
[6] Couto, C., Real, P.V. (2019). On the interaction between local and lateral-torsional buckling of I-shaped slender section beams. Proceedings of the Annual Stability Conference Structural Stability Research Council St. Louis, Missouri.
[7] Sener, K., Witte, J., Varma, A.H. (2019). On the influence of load width on web compression buckling strength. Proceedings of the Annual Stability Conference Structural Stability Research Council St. Louis, Missouri, pp. 1-13.
[8] Mamazizi, S., Crocetti, R., Mehri, H., University, L. (2013). Numerical and Experimental Investigation on the Post-Buckling Behavior of Steel Plate Girders Subjected to Shear. Proceedings of the Annual Stability Conference Structural Stability Research Council St. Louis, Missouri, pp. 739-749.
[9] Witte, J. (2019). Influence of loading width on web compression buckling of steel beams. Master Thesis, Lyles School of Civil Engineering, Purdue University.
[10] Topkaya, C. (2006). A numerical study on linear bifurcation web buckling of steel I-beams in the sidesway mode. Eng Struc 28, pp. 1028–1037. DOI: https://doi.org/10.1016/j.engstruct.2005.11.009.
[11] Sediek, O.A., Safar, S.S., Hassan, M.M. (2024). Imperfect tapered plate girder web under shear. Int J Steel Struct 24, pp. 431–445. DOI: https://doi.org/10.1007/s13296-024-00826-7.
[12] Ammash, H.K., Shaffaf, N.N. (2023). Behavior study of the steel plate girder with a cellular honeycomb web. Scientific Review Eng and Envir Sci 32, pp. 101–116. DOI: https://doi.org/10.22630/srees.4743.
[13] Abbas, J.L. (2023). Behaviour of Steel I Beams with Web Openings. Civ Eng J 9, pp. 596–617. DOI: https://doi.org/10.28991/CEJ-2023-09-03-08.
[14] Al-Mazini, M. (2016). Effect of Web Opening on the Ultimate Capacity of Steel Plate Girders under Two Points Load. Eng and Tech J, 34, 165–177. DOI: https://doi.org/10.30684/etj.34.1A.14.
[15] El-Dehemy, H., 2017. Static and Dynamic Analysis Web Opening of Steel Beams. World J Eng Tech 05, pp. 275–285. DOI: https://doi.org/10.4236/wjet.2017.52022.
[16] Hamed, A. (2023). Elastic shear buckling of tapered steel plate girders with opening in web. J Eng Sci, Vol. 51, No. 3, pp. 148-172. DOI: https://doi.org/10.21608/jesaun.2023.177464.1184.
[17] Niu, S., R. Rasmussen, K.J., Fan, F. (2015). Local–Global Interaction Buckling of Stainless Steel I-Beams. I: Experimental Investigation. J. Struct. Eng. 141, 04014194. DOI: https://doi.org/10.1061/(ASCE)ST.1943-541X.0001137.
[18] Park, J.S., Stallings, J.M. (2003). Lateral-Torsional Buckling of Stepped Beams. J. Struct. Eng. 129, pp. 1457–1465. DOI: https://doi.org/10.1061/(ASCE)0733-9445(2003)129:11(1457).
[19] Surla, A.S., Kang, S.Y., Park, J.S. (2015). Inelastic buckling assessment of monosymmetric I-beams having stepped and non-compact flange sections. J Constr Steel Res 114, pp. 325–337. DOI: https://doi.org/10.1016/j.jcsr.2015.08.019.
[20] Alolod, S., Park, J., Won, D. (2020). Lateral Torsional Buckling Strengths of Stepped Beams at Midspan Exposed to Elevated Temperature. Int J Steel Struct 20, pp. 2028–2037. DOI: https://doi.org/10.1007/s13296-020-00427-0.
[21] Reichenbach, M.C., Liu, Y., Helwig, T.A., Engelhardt, M.D. (2020). Lateral-Torsional Buckling of Singly Symmetric I-Girders with Stepped Flanges. J. Struct. Eng. 146, 04020203. DOI: https://doi.org/10.1061/(ASCE)ST.1943-541X.0002780.
[22] Trinh, D.K., Nguyen, D.H., Bui, H.C., Nguyen, M.T. (2023). Lateral torsional buckling of I-section simply supported beams with stepped height. Steel Constr. 202300020. DOI: https://doi.org/10.1002/stco.202300020.
[23] Almasri, A.H., Jabur, I. (2024). Assessing lateral torsional buckling of stepped steel I beams using finite element method. Forces in Mechanics 15, 100266. DOI: https://doi.org/10.1016/j.finmec.2024.100266.
[24] Mecway FEA version 16, (2022). Finite element analysis package for Windows with a focus on mechanical and thermal simulation. https://mecway.com.
[25] ANSI/AISC 360-16. Specification for structural steel buildings. Chicago: American Institute of Steel Construction (AISC), 2016.
[26] BS EN 1993-1-5. Eurocode 3: Design of steel structures: Part 1–5: Plated structural elements. London: British Standard Institution (BSI), 2006.

[27] Holtz, N.M., Kulak, G.L., 1975. Structural Engineering Report No. 51. University of Alberta, Edmonton, Alberta, Canada.
[28] https://www.timesunion.com/news/article/construction-albany-county-rail-trail-bridge-18197215.php. Last accessed in 15/6/2025.
[29] https://www.timesunion.com/news/article/albany-county-releases-report-rail-trail-bridge-18353527.php. Last accessed in 15/6/2025.